Controlled Contact to a C_{60} Molecule

N. Néel,[1] J. Kröger,[1,*] L. Limot,[1,†] T. Frederiksen,[2] M. Brandbyge,[2] and R. Berndt[1]

[1]*Institut für Experimentelle und Angewandte Physik, Christian-Albrechts-Universität zu Kiel, D-24098 Kiel, Germany*

[2]*MIC—Department of Micro and Nanotechnology, NanoDTU, Technical University of Denmark, DK-2800 Kongens Lyngby, Denmark*

(Received 22 August 2006; published 7 February 2007)

The tip of a low-temperature scanning tunneling microscope is approached towards a C_{60} molecule adsorbed at a pentagon-hexagon bond on Cu(100) to form a tip-molecule contact. The conductance rapidly increases to ≈ 0.25 conductance quanta in the transition region from tunneling to contact. *Ab-initio* calculations within density functional theory and nonequilibrium Green's function techniques explain the experimental data in terms of the conductance of an essentially undeformed C_{60}. The conductance in the transition region is affected by structural fluctuations which modulate the tip-molecule distance.

DOI: 10.1103/PhysRevLett.98.065502 PACS numbers: 61.48.+c, 68.37.Ef, 73.63.Rt

The mechanical and electronic properties of materials at the atomic scale are important in various research areas ranging from adhesion and friction to photosynthesis and signal transduction in molecular structures. Electronic transport through nanostructures may find applications in devices and is being investigated for semiconducting [1] and metallic [2,3] constrictions, carbon nanotubes [4], DNA [5–8], and single metal atoms [9].

Scanning tunneling microscopy (STM) appears to be an ideal tool to study single-molecule conductance in detail. The structure under investigation—a molecule along with its substrate—can be imaged with submolecular precision prior to and after taking conductance data. Parameters such as molecular orientation or binding site, which are expected to significantly affect conductance properties, can thus be monitored. Moreover, specific parts of a molecule may be addressed to probe their role in electron transport, signal transduction, or energy conversion. Another advantage of STM is the possibility to characterize to some extent the status of the second electrode, the microscope tip, by recording conductance data on clean metal areas. Consequently, STM can complement techniques like the mechanically controlled break-junction measurements.

Scanning probe techniques have indeed been used to form point contacts between the tip and a metal surface whose quantized conductance was then investigated during forming and stretching of the contact [10–12]. Taking advantage of the imaging capability of STM a recent experiment on contacts to single adsorbed atoms (adatoms) [9] showed that tip-adatom contacts can be formed reproducibly without structural changes of tip or sample. Somewhat surprisingly, STM data for molecular point contacts are scarce. Joachim *et al.* used STM at ambient temperature to study the contact conductance of a C_{60} on Au(110) [13].

Here we present low-temperature STM measurements of the conductance ($G = I/V$; I is the current, V is the sample voltage) of C_{60} molecules adsorbed on Cu(100). These favorable conditions enable identification of individual molecule orientations which facilitates the comparison of experimental data with model calculations. Images prior to and after contact showed that the C_{60} molecules as well as the tip status remain unchanged despite the large currents applied (up to 30 μA). The transition from the tunneling to the contact regime is signaled by a rapid rise of the conductance to $G \approx 0.25G_0$, where $G_0 = 2e^2/h$. When approaching the tip further towards the molecule a jump up to $G \approx G_0$ is observed. The experimental data are modeled with density functional theory (DFT) and nonequilibrium Green's function techniques. Our theory captures the important characteristics of the experiment and explains the underlying physics. Experimental and theoretical findings differ from those reported for C_{60} on Au(110) [13].

The experiments were performed with a scanning tunneling microscope operated at 8 K and in ultrahigh vacuum at a base pressure of 10^{-9} Pa. The Cu(100) surface as well as chemically etched tungsten tips were cleaned by annealing and argon ion bombardment. C_{60} was evaporated from a tantalum crucible while keeping the residual gas pressure below 5×10^{-8} Pa. An ordered C_{60} superstructure was obtained by deposition onto the clean surface at room temperature and subsequent annealing to 500 K. Deposition rates were calibrated with a quartz microbalance to be $\approx$1 ML min^{-1}. We define a monolayer (ML) as one C_{60} molecule per 16 copper atoms. The tungsten tip was controllably indented into pristine Cu surface areas until C_{60} images exhibited submolecular resolution (Fig. 1) and dI/dV spectra on the Cu surface were featureless. Given this preparation, the tip is covered with substrate material. While these tips lead to data as presented in Fig. 2, blunt tips exhibit larger contact conductances. We made sure that in spite of the unusually high currents no significant voltage drop at the input impedance of the current-to-voltage converter occurred. Thus, the decrease of the bias voltage at the tip-molecule junction was negligible.

A constant-current STM image of annealed Cu(100)-C_{60} is shown in Fig. 1. The molecules are arranged in a hexagonal lattice and exhibit a superstructure of bright

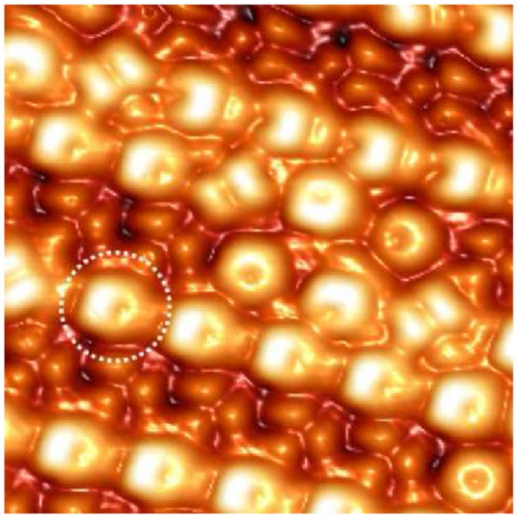

FIG. 1 (color online). Pseudo-three-dimensional representation of a constant-current STM image of Cu(100)-C_{60} at 8 K. (Sample voltage $V = 1.7$ V, tunneling current $I = 1$ nA, scan size 49 Å $\times$ 49 Å). A dashed circle indicates the C_{60} orientation on which we performed the conductance measurements.

and dim rows which is associated with a missing-row reconstruction of the copper surface [14]. Bright rows correspond to C_{60} molecules in a missing Cu row while dim rows correspond to molecules located at double missing rows. Figure 1 exhibits, similar to the case of C_{60} on Ag(100) [15], four molecular orientations on Cu(100).

To study theoretically the Cu(100)-C_{60} system in the presence of an STM tip we use the SIESTA [16] and TRANSIESTA [17] DFT packages [18]. The system is modeled by a periodic supercell containing one C_{60} molecule

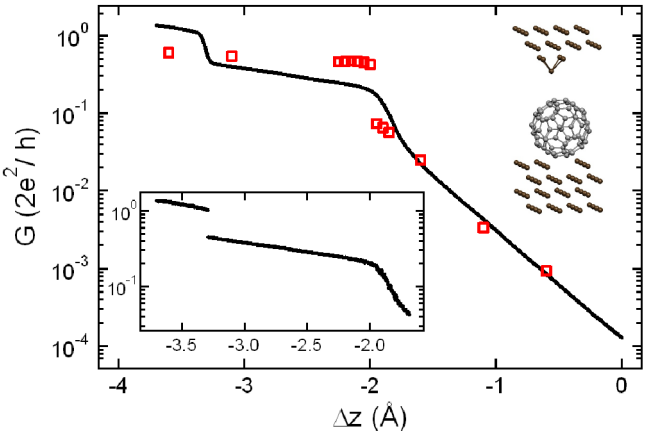

FIG. 2 (color online). Conductance G in units of G_0 vs tip displacement Δz. Data are an average of 500 measurements. Zero displacement corresponds to the tip position before freezing the feedback loop at $V = 300$ mV and $I = 3$ nA. Experimental data appear as a line due to the high data point density, calculated data are depicted as squares. Upper inset: setup for calculations. Lower inset: single conductance curve revealing a discontinuity at $\Delta z \approx -3.3$ Å.

on a 4×4 representation of six Cu(100) layers with a single missing-row surface. The tip is represented by a Cu pyramid mounted on the reverse side of the surface film. This setup is illustrated in the upper inset of Fig. 2. To determine the microscopic arrangement at different tip-substrate distances we gradually diminish the length of the supercell in the direction perpendicular to the surface and relax both C_{60} and tip atoms until all residual forces on these atoms are smaller than 0.02 eV/Å. The conductance is finally determined from a calculation of the zero-bias transmission function of the junction by including DFT self-energies for the coupling to semi-infinite atomistic leads.

In the following we discuss electron transport measurements through an individual C_{60} of the 5:6 type; i.e., the molecule is oriented such as to exhibit a carbon-carbon bond between a carbon pentagon and a carbon hexagon at the top (see the molecule encircled by a dashed line in Fig. 1). Calculations for other molecular configurations are in progress. Figure 2 presents experimental (dots) and calculated (squares) results for the conductance G (in units of G_0) on a logarithmic scale. Because of their large number ($\approx$1150) experimental data points overlap and appear as a line. The displacement axis shows the tip excursion towards the molecule with $\Delta z = 0$ corresponding to the position of the tip before opening the feedback loop of the microscope. The tip is then moved towards the molecule ($\Delta z < 0$) by more than 3.5 Å while the current is simultaneously recorded to explore the evolution of the conductance of the tip-molecule junction in a range of distances between the tip and the molecule. Conductance curves recorded at voltages between 50 mV and 600 mV revealed a similar shape.

Typical characteristics of the conductance curve are as follows. Between $\Delta z = 0$ and $\Delta z \approx -1.6$ Å the conductance varies exponentially from $10^{-4}G_0$ to $\approx 0.025G_0$ consistent with electron tunneling from tip to sample states. Starting from $\Delta z \approx -1.6$ Å we observe deviations from the exponential behavior. A sharp increase of the conductance by a factor of 10 to $\approx 0.25G_0$ occurs within a displacement interval of $\approx$0.4 Å. For comparison, in the tunneling regime this displacement leads to an increase of the conductance by only a factor of 3.5. We find that the width of the transition region is voltage dependent. Further decrease of the tip-molecule distance increases the conductance although the slope is reduced by a factor of 10 compared to the tunneling regime. At a displacement of $\Delta z \approx -3.3$ Å a second rapid increase of the conductance to G_0 is observed. This rise is discontinuous at the resolution of the experiment as can be seen from a single, unaveraged conductance trace (lower inset of Fig. 2). Because of the small variation in the exact location of this jump, averaging over 500 instances leads to some broadening. Upon further approach, the conductance exhibits yet another very small increase with decreasing tip-

molecule distance. For for tip excursions $\Delta z < -3.8$ Å instabilities and damage of the tip or sample were often observed.

The results of our calculations (squares in Fig. 2) describe most of the essential features of the experimental conductance data. To compare with experimental data the calculated conductance curve was shifted along the displacement axis until experimental and calculated tunneling regions coincided. The tunneling regime is reproduced with the experimentally measured slope. A rapid increase of the conductance occurs at $\Delta z \approx -2.0$ Å, leading to a conductance which is comparable to the experimental value and clearly lower than G_0 [19]. This rise of the conductance can be understood from the relaxed tip-molecule geometries. As the electrode separation is reduced by only 0.05 Å, the tip-molecule distance shrinks from 3.18 Å to 2.34 Å. This results in the formation of a chemical bond between the tip apex and the C_{60} which hence effectively closes the tunneling gap. Concomitantly, the conductance increases by a factor of 6. Around this instability point—which defines the transition from tunneling to contact—we find that only small energy differences discriminate between the configurations with or without the tip-molecule bond. This is shown in Fig. 3(a) where the calculated zero-temperature data points are seen to fall on one of two straight lines that correspond to either a tunneling (smaller slope) or a contact (larger slope) configuration of the junction. At finite temperatures and under the nonequilibrium conditions imposed by the bias voltage, it is therefore likely that the junction will fluctuate between these different situations. From a couple of data points just before (after) the conductance jump we can extrapolate the distance dependence of the conductance G_t (G_c) and total energy E_t (E_c) corresponding to a tunneling (contact) configuration. With these at hand we can establish the thermally averaged conductance over a fluctuation between these two situations according to

$$\bar{G}(\Delta z) = \frac{G_t(\Delta z)e^{-\beta E_t(\Delta z)} + G_c(\Delta z)e^{-\beta E_c(\Delta z)}}{e^{-\beta E_t(\Delta z)} + e^{-\beta E_c(\Delta z)}},$$

where $\beta = 1/k_B T$ is the inverse temperature (k_B: Boltzmann's constant). The results of this procedure are shown in Fig. 3(b) with dashed lines corresponding to two different values for the effective temperature. With the temperature of the cryostat ($T = 8$ K) a sharp transition from tunneling to contact is predicted to occur around $\Delta z = -1.87$ Å. The position of this jump agrees very well with that of the experimental data but its width is too narrow. However, if the effective temperature is increased to $T = 400$ K the experimental width of the transition region is well reproduced by our calculations. From an estimate of the maximal energy dissipation in the junction at the given bias voltage we find that this effective temperature is plausible [20]. Further, the evaluated relative variation of experimentally acquired conductances

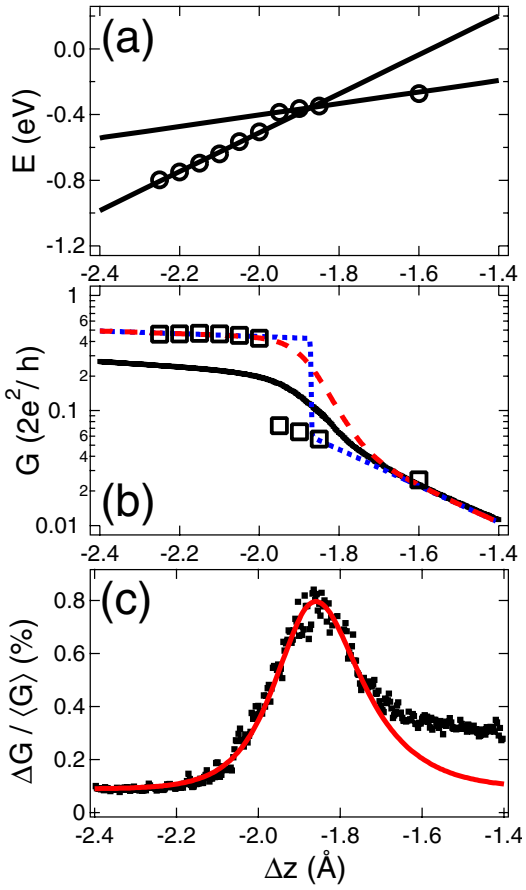

FIG. 3 (color online). (a) Calculated total energy differences vs tip displacement Δz in the transition region from tunneling to contact. The data points (○) fall on one of two straight lines corresponding to either a tunneling (smaller slope) or a contact (larger slope) configuration. (b) Experimental (●) and theoretical (squares and dashed lines) conductance data in the tunneling-contact transition regime. Thin and thick dashed lines represent the theoretical conductance corresponding to a thermal average for a fluctuation between tunneling and contact configurations with $T = 8$ K and $T = 400$ K, respectively (see text). (c) Ratio of the standard deviation ΔG over the mean conductance $\langle G \rangle$ evaluated over 500 conductance curves within the tunneling-contact transition regime. Full line: calculated data for an effective temperature of 400 K (divided by 200 to be plotted on the same axis as experimental data).

exhibits a maximum in the transition regime from tunneling to contact [see Fig. 3(c)] pointing at structural fluctuations which modulate the tip-molecule distance and thus the conductance. Except for absolute values this curve can be reproduced by our calculations. Additionally, the width of the transition depends on the bias voltage, i.e., on the energy dissipation in the junction. These observations are strong indications that the fluctuation interpretation is correct.

Comparing our results for C_{60} on Cu(100) with those obtained by Joachim *et al.* [13] for C_{60} on Au(110) we find similar trends in both experiments. However, there are

some differences to be discussed next. Taking $G = 1.3 \times 10^{-4} G_0$, which is located in the tunneling regime (Fig. 2), as a reference point, we observe an exponential tunneling behavior for G over a range of 1.6 Å, after which G enters the tunneling-contact transition region at $\approx 2.5 \times 10^{-2} G_0$. In Ref. [13], the transition region is already reached at $2.5 \times 10^{-4} G_0$. We hint that this difference may be caused by thermally induced molecule rotations. While in our experiment G reaches G_0 at $\Delta z \approx -3.3$ Å with a discontinuous jump, no jump was reported in Ref. [13] and G is still smaller than G_0 for displacements as large as -10 Å. The discontinuous conductance change is likely due to a sudden rearrangement of the tip or molecule adsorption geometry leading to a higher number of conductance channels. The calculations of Ref. [13] suggest that the C_{60} cage collapses upon contact, whereas in our model the deformation of the C_{60} molecule in contact with the tip is small. The molecule remains almost spherical with only small relaxations of the carbon-carbon bond lengths (the diameter of the cage changes by less than 4%). The accelerated rise of the conductance is attributed to splitting of the molecular levels of the C_{60} molecule upon strong compression in Ref. [13], while we argue that the rise is due to an increased electronic coupling between the tip and the molecule when they form a bond.

Possible reasons for the above differences are as follows. The different substrate materials used affect the C_{60}-metal bond. The absence of intramolecular resolution at room temperature is a hint for thermally induced molecule rotation. Therefore, in an ambient temperature experiment averaging over a number of molecular orientations is likely to occur. At low temperature a single geometry is probed. Finally, the interpretations of Ref. [13] rely on more approximate molecular mechanics modeling (MM2) and do not take the significant deformation of the tip into account.

In conclusion, we used low-temperature STM and theoretical modeling to investigate contacts to a C_{60} molecule on Cu(100). In the experiment, the junction is stable up to currents of 30 μA and reproducible conductance data are obtained. When approaching the microscope's tip, deviations from tunneling are observed similar to those observed from single adatoms which are due to deformations of the tip. At contact, we find a conductance of $G \approx 0.25 G_0$. Further decrease of the gap spacing leads to a discontinuous conductance change to $G \approx G_0$. From our modeling we infer that the controlled contact to a C_{60} molecule does not significantly deform its spherical shape. Moreover, we show that the conductance around the tip-molecule contact formation is affected by a fluctuation between different microscopic configurations.

We thank C. Cepek (Laboratorio Nazionale TASC, Italy) for providing C_{60}, the Deutsche Forschungsgemeinschaft for financial support through SPP 1153, and the Danish Center for Scientific Computing (DCSC) for computational resources.

*Electronic address: kroeger@physik.uni-kiel.de
†Present address: Institut de Physique et Chimie des Matériaux de Strasbourg, UMR 7504, Université Louis Pasteur, 23 rue du Loess, F-67034 Strasbourg, France.

[1] B. J. van Wees, H. van Houten, C. W. J. Beenakker, J. G. Williamson, L. P. Kouwenhoven, D. van der Marel, and C. T. Foxon, Phys. Rev. Lett. **60**, 848 (1988).
[2] C. J. Muller, J. M. van Ruitenbeek, and L. J. de Jongh, Phys. Rev. Lett. **69**, 140 (1992).
[3] E. Scheer, P. Joyez, D. Esteve, C. Urbina, and M. H. Devoret, Phys. Rev. Lett. **78**, 3535 (1997).
[4] S. Frank, P. Poncharal, Z. L. Wang, and W. A. de Heer, Science **280**, 1744 (1998).
[5] M. Rief, M. Gautel, F. Oesterhelt, J. M. Fernandez, and H. E. Gaub, Science **276**, 1109 (1997).
[6] H.-W. Fink and C. Schönenberger, Nature (London) **398**, 407 (1999).
[7] D. Porath, A. Bezryadin, S. de Vries, and C. Dekker, Nature (London) **403**, 635 (2000).
[8] A. Y. Kasumov, M. Kociak, S. Guéron, B. Reulet, V. T. Volkov, D. V. Klinov, and H. Bouchiat, Science **291**, 280 (2001).
[9] L. Limot, J. Kröger, R. Berndt, A. Garcia-Lekue, and W. A. Hofer, Phys. Rev. Lett. **94**, 126102 (2005).
[10] J. K. Gimzewski and R. Möller, Phys. Rev. B **36**, 1284 (1987).
[11] J. I. Pascual, J. Méndez, J. Gómez-Herrero, A. M. Baró, N. García, and V. T. Binh, Phys. Rev. Lett. **71**, 1852 (1993).
[12] L. Olesen, E. Lægsgaard, I. Stensgaard, F. Besenbacher, J. Schiøtz, P. Stoltze, K. W. Jacobsen, and J. K. Nørskov, Phys. Rev. Lett. **72**, 2251 (1994).
[13] C. Joachim, J. K. Gimzewski, R. R. Schlittler, and C. Chavy, Phys. Rev. Lett. **74**, 2102 (1995).
[14] M. Abel, A. Dimitriev, R. Fasel, N. Lin, J. V. Barth, and K. Kern, Phys. Rev. B **67**, 245407 (2003).
[15] X. Lu, M. Grobis, K. H. Khoo, S. G. Louie, and M. F. Crommie, Phys. Rev. Lett. **90**, 096802 (2003).
[16] J. M. Soler, E. Artacho, J. D. Gale, A. García, J. Junquera, P. Ordejón, and D. Sánchez-Portal, J. Phys. Condens. Matter **14**, 2745 (2002).
[17] M. Brandbyge, J. L. Mozos, P. Ordejón, J. Taylor, and K. Stokbro, Phys. Rev. B **65**, 165401 (2002).
[18] Electronic structure calculations are based on the generalized gradient approximation for the exchange-correlation functional, a single-ζ plus polarization basis for the valence electrons, a 200 Ry cutoff energy for the real space grid integrations, and the Γ-point approximation. Core electrons are described with pseudopotentials. The conductance is calculated from the zero-bias transmission at the Fermi energy sampled over 3×3 **k** points in the two-dimensional Brillouin zone in the transverse plane of the transport.
[19] The small quantitative difference between theory and experiment for the contact conductance might be related to tip shape and tip position over the C_{60} molecule.
[20] M. Paulsson, T. Frederiksen, and M. Brandbyge, Nano Lett. **6**, 258 (2006).